Microporous and Mesoporous Materials 143 (2011) 87–96

Contents lists available at ScienceDirect

Microporous and Mesoporous Materials

journal homepage: www.elsevier.com/locate/micromeso

FTIR and ^{27}Al MAS NMR analysis of the effect of framework Al- and Si-defects in micro- and micro-mesoporous H-ZSM-5 on conversion of methanol to hydrocarbons

Petr Sazama [a,*], Blanka Wichterlova [a], Jiri Dedecek [a], Zdenka Tvaruzkova [a], Zuzana Musilova [a], Luisa Palumbo [b], Stepan Sklenak [a], Olga Gonsiorova [a,1]

[a] J. Heyrovský Institute of Physical Chemistry, Academy of Sciences of the Czech Republic, CZ-182 23 Prague 8, Czech Republic
[b] Dipartimento di Chimica IFM-NIS Centre of Excellence, Università di Torino, Via P. Giuria 7, 10125 Torino, Italy

ARTICLE INFO

Article history:
Received 3 January 2011
Received in revised form 7 February 2011
Accepted 8 February 2011
Available online 13 February 2011

Keywords:
Micro-mesoporous H-ZSM-5 zeolite
Framework defects
FTIR
^{27}Al MAS NMR
Methanol to hydrocarbons (MTH)

ABSTRACT

A series of micro- and micro-mesoporous H-ZSM-5 zeolites with highly regular and, on the other side, a defective framework were prepared by synthesis and post-synthesis treatment, and their activity was investigated in transformation of methanol to low olefins, aromatics and paraffins. ^{27}Al MAS NMR and FTIR spectroscopy of OH groups and C≡N groups of adsorbed d_3-acetonitrile were used for analysis of the population of framework Al- and Si-related defective sites. Beside framework Al atoms in regular Td coordination, perturbed Td coordinated Al atoms and partly extra-framework Al species, and the internal Si–OH groups as Si-related defects were identified. The increase in the concentration of framework Al- and Si-defective sites in microporous H-ZSM-5 was manifested in methanol transformation in the increased yields of aromatics and paraffins, while highly regular framework preferred formation of low C_2 and C_3 olefins. The non-defective micro-mesoporous H-ZSM-5 prepared by alkaline and subsequent oxalic acid leaching of the zeolite with silanols typical for external crystal surface gave substantially longer catalyst life-time. The micro-mesoporous H-ZSM-5 (synthesized by using carbon particles) exhibited high content of defective sites, i.e., inner silanols, interacting OH groups, perturbed framework Al atoms and Al-Lewis sites, provided a slight increase in the yield of paraffins and C_6^+ aromatics, and particularly much lower catalyst life-time compared to the sample of similar composition and synthesis procedure carried out without carbon presence. These findings point out on the importance of highly regular framework of H-ZSM-5 for methanol to olefin transformation, and on the way of preparation of micro-mesoporous H-ZSM-5 by desilication with alkaline solution followed by acid leaching of electron acceptor sites, resulting in the high life-time of the catalyst.

1. Introduction

The process of conversion of methanol to hydrocarbons (MTH) over H-ZSM-5 zeolites, developed by Mobil Oil Co., in 1970s, is an alternative route for production of hydrocarbons independent of crude oil [1,2]. MTH converts methanol to a mixture of olefins, paraffins, and alkylaromatics, with the aim to produce either hydrocarbon mixtures rich in the gasoline fraction (MTG) or low chain olefins (MTO) [3,4]. As feedstock requirements for production of polymers are continuously growing and diesel fuel is coming more into demand than gasoline, there is a growing interest for conversion of methanol to C_2 and C_3 olefins. However, the MTH processes in general suffer from problems of selectivity and catalyst deactivation/regeneration.

The ZSM-5 zeolite (MFI topology) possesses tri-dimensional pore structure of straight channels (5.6 × 5.3 A) and intersecting zig–zag channels (5.5 × 5.1 A), which are accessible for diffusion of $<C_9$ aromatic molecules. As the strength of acidic structural OH groups of H-ZSM-5 is independent on the Al content in the framework [5–9], methanol transformation over H-ZSM-5, typically a process with consecutive reaction steps, is driven mainly by the concentration of the zeolite protons and the dimension and architecture of the free inner volume. The MTH process over structurally stable H-ZSM-5 needs to increase selectivity to olefins for the MTO process as well as catalyst life-time.

MTH process relies on the "hydrocarbon pool" mechanism, in which methanol reacts with entrained hydrocarbon species in the zeolite pores, olefins and alkyl aromatics, and the alkylation, isomerisation, cracking and hydrogen transfer reactions take place

* Corresponding author.
E-mail address: petr.sazama@jh-inst.cas.cz (P. Sazama).
[1] Present address: Euro Support Manufacturing Czechia, s.r.o., 436 70 Litvínov-Záluží 1, Czech Republic.

1387-1811/$ - see front matter © 2011 Elsevier Inc. All rights reserved.
doi:10.1016/j.micromeso.2011.02.013

(see *e.g.*, Refs. [2,3,10–21] and references therein). Beside the concentration of strong acid structural OH groups, the regular pore dimensions of ZSM-5 structure governs the shape selectivity effect of the inner reaction space by limiting the over-alkylation and formation of polyaromatics and thus controls formation of bulky polyalkyl aromatics. Formation of these deposits occurs at a crystal surface and partly inside channels, and they increasingly block the acid sites and limit the mass transport of reactants and products [17,22].

It has been shown that the mass transport through the zeolite crystal can be basically enhanced by using crystals of nano-size dimension and/or by the incorporation of mesopores. The mesoporosity can be produced by zeolite desilication with alkaline solutions [23–29] or dealumination by acids [30,31], or by introduction of secondary template species, like carbon particles at the synthesis step, which are thereafter burned off to yield crystalline micro-mesoporous hierarchical structure [31–38]. Network of mesopores inter-connected with the crystal surface and thus easily accessible to reactants results in enhanced diffusivity through the zeolite crystals [26]. On the contrary, intra-crystalline mesopores surrounded by the micropore crystalline solid, do not significantly affect intra-crystalline diffusion [39], but might represent large cavities from which products diffuse out with difficulty.

Groen et al. in a feature article [24] described main principles of mesopore formation in H-ZSM-5 crystals by their alkaline leaching. They stressed for such desilication, beside the temperature and concentration of the alkaline solution, the importance of Si/Al composition. They suggested that the presence of framework Al atoms stabilizes a neighbouring siliceous part of the crystal. The mesopores formed in large ZSM-5 crystals (17 μm) by alkaline desilication were manifested in an enhanced diffusion of 2 orders of magnitude through the micro-mesoporous ZSM-5 [26]. The benefit of micro-mesoporous structure obtained by desilication was also demonstrated on a substantial increase in the catalyst life-time with large H-ZSM-5 crystals (15 μm), which originally do not exhibit long reaction performance [40]. Analysis of the location and type of acid sites by adsorption of CO and voluminous collidine revealed that besides desilication, the Al-Lewis sites are formed, preferably in the mesopores [9]. Jacobsen et al. [32] introduced secondary mesoporosity in ZSM-5 using carbon nanoparticles encapsulated during synthesis in the zeolite crystals and subsequently removed by controlled combustion. The obtained micro-mesoporous zeolite exhibited improved activity and selectivity in alkylation of benzene compared to a conventional microporous H-ZSM-5 [41].

Because of the high importance of the selectivity to olefins or aromatics for the MTH processes, and of the extent of zeolite coking, it should be considered if any perturbations (defects) of the crystalline structure, either strictly local or more massive, like mesopores, would significantly affect both the nature and amount of the active sites (protons and Al-related electron acceptors).

In the present work, we analyse the effect of low concentration of Si- and Al-related framework perturbations (defects) in the regular framework of small crystals of microporous and micro-mesoporous H-ZSM-5 on their activity, selectivity and life-time in methanol transformation to hydrocarbons. ^{27}Al MAS NMR, FTIR spectra of OH groups and C≡N groups of adsorbed d_3-acetonitrile and nitrogen sorption measurements are employed to identify the structure and content of tetrahedrally coordinated aluminium atoms in the framework connected with structural Si–OH–Al groups, of perturbed environment of framework Al atoms, Al–OH groups, Al-Lewis electron acceptor sites, and internal and external Si–OH groups.

2. Experimental

2.1. Preparation of ZSM-5 zeolites

Table 1 lists ZSM-5 zeolites, both commercial samples and those synthesized in the laboratory. *M* denotes microporous and *MM* micro-mesoporous zeolites. Sample Z-25/M with Si/Al 25 was purchased from Conteca and sample Z-27.5/M with Si/Al 27.5 was supplied by ALSI-PENTA Zeolithe GmbH. Samples Z-37.5/MM, Z-38/M, Z-45/M and Z-48/MM with Si/Al 37.5, 38, 45 and 48, respectively were synthesized in our laboratory. Z-45/M was synthesized by using TPAOH as a structure-directing agent, and $Al(NO_3)_3{\cdot}9H_2O$ and TEOS as sources of aluminium and silicon, respectively. The crystallization was performed under static conditions for 6 days at autogeneous pressure at a temperature of 170 °C in a Teflon-lined autoclave. Micro-mesoporous ZSM-5 sample Z-48/MM was prepared by using carbon black CBP2000 (CS Cabot Corporation, Czech Republic) as a secondary template to TPAOH, and the synthesis procedure was analogous to Z-45/M. The template and carbon black were simultaneously removed by calcination in a static air at 550 °C for 6 h. The synthesis of ZSM-5/38/M was performed by using TPAOH as a template with TPA/Si molar ratio of 0.008. Sources of aluminium and silicon were precipitated at a controlled pH and mixed for 24 h at RT. The crystallization was performed in an autoclave with agitation at a temperature of 160 °C for 8 h under autogeneous pressure. The template was removed from the zeolites by calcination in a static air at 550 °C for 6 h. Z-37.5/MM was obtained by alkaline leaching of Z-38/M followed by acid treatment in two steps: (i) 1 g of Z-38/M was poured into 100 cm^3 of 0.065 mol dm^{-3} NaOH at 80 °C and stirred for 20 h. The zeolite suspension was then repeatedly centrifuged and re-dispersed in distilled water. The washed solid phase was dried at 80 °C; (ii) the zeolite obtained by NaOH leaching was poured into an aqueous solution of oxalic acid (1 g of the sample per 42 cm^3 of 2.5 mol dm^{-3} oxalic acid) and stirred at 80 °C for 10 h. The zeolite suspension was then repeatedly centrifuged and re-dispersed in distilled water. The solid was dried at 80 °C.

Table 1
Characteristics of ZSM-5 zeolites.

Sample	Crystal size (μm)	Si/Al[a]	c_{Al}[a] (mmol g^{-1})	c_B[b] (mmol g^{-1})	c_L[c] (mmol g^{-1})	$c_B + 2c_L$ (mmol g^{-1})
Z-25/M[d]	0.5	25	0.63	0.43	0.08	0.59
Z-27.5/M[d]	3	27.5	0.58	0.47	0.05	0.57
Z-37.5/MM[e]	0.5	37.5	0.43	0.33	0.04	0.41
Z-38/M[e]	0.5	38.0	0.42	0.36	0.01	0.38
Z-45/M[e]	0.5	45	0.36	0.19	0.07	0.33
Z-48/MM[e]	1	48	0.34	0.22	0.05	0.32

[a] From chemical analysis.
[b,c] Concentrations of Broensted and Lewis sites, respectively, from FTIR spectra of adsorbed d_3-acetonitrile.
[d] Commercial ZSM-5.
[e] ZSM-5 synthesized in the laboratory.

All the zeolites were ion-exchanged with 0.5 mol dm^{-3} NH_4NO_3 at RT (1 g of a zeolite per 100 cm^3 of solution, three times over 12 h). To obtain the Na^+ form for ^{27}Al MAS NMR measurements, the zeolites were ion-exchanged with 0.5 M $NaNO_3$ at RT (100 ml of solution per 1 g of a zeolite applied three times over 8 h). After the NH_4^+ or Na^+ ion-exchange, the zeolites were carefully washed with distilled water and dried in the open air.

2.2. Characterization of ZSM-5 zeolites

The chemical composition of the zeolites was determined by Atomic Absorption Spectrometry after dissolution of the zeolite samples (Table 1). The structure and crystallinity of the samples were checked by X-ray powder diffraction analysis on a Siemens 5005 diffractometer using Cu Kα radiation and a graphite monochromator. ^{27}Al MAS NMR experiments of Na^+-forms of zeolites were performed on a Bruker Avance 500 MHz (11.7 T) Wide Bore spectrometer using 4 mm o.d. ZrO_2 rotors with a rotation speed of 12 kHz. Proton high-power decoupling pulse sequences with π/6 (1.4 μs) excitation pulses were employed to allow quantitative evolution of the ^{27}Al MAS NMR spectra. To determine the amount of the "invisible" extra-framework Al atoms rotors with the Na^+-zeolite samples were weighted before the spectra collection and the integrated intensity of the ^{27}Al signal was compared with that of the standard sample with the exclusive presence of Al atoms in the framework. Spectra were simulated using MestRec software. The chemical shifts were referenced to an aqueous solution of $Al(NO_3)_3$. Nitrogen sorption isotherms of ZSM-5 zeolites were measured with a Micromeritics ASAP 2020 volumetric instrument at −196 °C equipped with pressure transducers covering the 133 Pa, 1.33 and 133 kPa ranges. Prior to the sorption measurements, all the samples were degassed at 250 °C for at least 24 h until a pressure of 10^{-3} Pa. The concentration of acidic Brønsted and Lewis sites in H-ZSM-5 was determined from quantitative analysis of the characteristic IR bands of the C≡N vibrations at 2298 and 2325 cm^{-1}, respectively, of adsorbed d_3-acetonitrile on zeolites evacuated at 450 °C; for extinction coefficients see Ref. [42]. Adsorption of d_3-acetonitrile (13 mbar) was carried out at 298 K with subsequent evacuation for 15 min at the same temperature. The FTIR spectra were recorded on a Nicolet Magna 550 FTIR spectrometer operating at resolution of 2 cm^{-1} by collecting 200 scans for a single spectrum.

2.3. Catalytic experiments

H-zeolites in the form of 0.3–0.5 mm grains (typical weight 60 mg) were calcined prior to the test in an oxygen stream at 500 °C for 2 h. The methanol transformation was carried out in a fixed-bed through-flow reactor at 370 °C, atmospheric pressure and WHSV of 20 h^{-1}. The feed contained 22 mol.% of methanol and rest of He. The reaction products were analyzed by an on-line connected gas chromatograph (GC Hewlett Packard 6090) by using an HP-Plot Q column (30 m × 0.53 mm × 40 μm film thickness) and a flame ionization detector (FID).

3. Results

3.1. Structure of ZSM-5 zeolites

The XRD patterns of the parent zeolites are characteristic for the structure of ZSM-5. The peak intensities and absence of the baseline drift in diffraction patterns of the as-synthesized and calcined ZSM-5 zeolites indicated their high crystallinity. The average crystal size of the samples, estimated from the SEM micrographs (Table 1), was in the range from 0.5 to 3 μm. The textural properties of microporous Z-38/M and Z-45/M samples and their micro-mesoporous analogues prepared by leaching with solutions of sodium hydroxide and oxalic acid (Z-37.5/MM), and by hydrothermal zeolite synthesis with the secondary carbon template (Z-48/MM), respectively, are summarized in Table 2. The ZSM-5 zeolites prepared by standard hydrothermal synthesis (Z-38/M and Z-45/M) displayed almost rectangular shape of the isotherm being typical for purely microporous material in contrast to Z-37.5/MM and Z-48/MM, possessing both micro- and mesoporous features. Compared to microporous ZSM-5 analogues, the micropore volume of both micro-mesoporous zeolites slightly decreased with formation of similar mesopore volumes of 0.15 and 0.12 $cm^3\ g^{-1}$ for Z-37.5/MM and Z-48/MM, respectively.

3.2. Analysis of ^{27}Al MAS NMR spectra

^{27}Al MAS NMR spectra of fully hydrated Na-ZSM-5 zeolites are depicted in Fig. 1. The strong signal with a chemical shift of about 55 ppm corresponds to the tetrahedrally co-ordinated Al atoms in oxygen environment and, thus, reflects framework Al atoms. Octahedrally coordinated extra-framework Al atoms characterized by a resonance at about 0 ppm were not observed for any Na-zeolite sample. Moreover, total intensity of the ^{27}Al NMR signal corresponded to the Al content in the samples within 5 rel. % of Al content. Thus, the amount of the extra-framework Al species, also possibly "invisible" in NMR, in all the Na-ZSM-5 zeolites was negligible. The maximum of the signal of the Td coordinated Al varied in the range of 53–56 ppm and only the low intensity was found at about 61 ppm. These features have been explained by different siting of Al atoms in the framework T sites [43–45], which varied by zeolite synthesis and Si/Al composition. In addition to these characteristic narrow signals, a broad signal of low intensity in the range of 50–30 ppm is present in the spectra of Z-25/M, Z-45/M and Z-48/MM. Details of the spectra of selected pairs of samples are given in Fig. 1B for comparison of their features: the microporous Z-27.5/M vs. Z-25/M, and Z-38/M vs. Z-45/M with a close Si/Al ratio, and the micro-mesoporous Z-37.5/MM (prepared by leaching), and Z-48/MM (prepared by carbon black templating) with their microporous analogues Z-38/M and Z-45/M, respectively. The intensity increase in the 50–30 ppm region has often been found in the ^{27}Al MAS NMR spectra of faujasite and pentasil ring zeolites after their steaming, when perturbation or partial release of framework Al atoms can be expected [46–51]. However, the assignment of these spectral components and the nature of the

Table 2
Textural properties of ZSM-5 samples.

Sample	Preparation	V_{ME}[a] ($cm^3\ g^{-1}$)	D_{ME}[b] (nm)	V_{MI}[c] ($cm^3\ g^{-1}$)
Z-38/M	Hydrothermal synthesis	–	–	0.16
Z-37.5/MM	Leaching of Z-38/M by NaOH and oxalic acid	0.15	13.5	0.14
Z-45/M	Hydrothermal synthesis	–	–	0.14
Z-48/MM	Synthesis with carbon template analogous to Z-45/M	0.12	18	0.13

[a] V_{ME} – mesopore volume.
[b] D_{ME} – mesopore diameter corresponding to the maximum of the pore size distribution.
[c] V_{MI} – micropore volume determined by t-plot method.

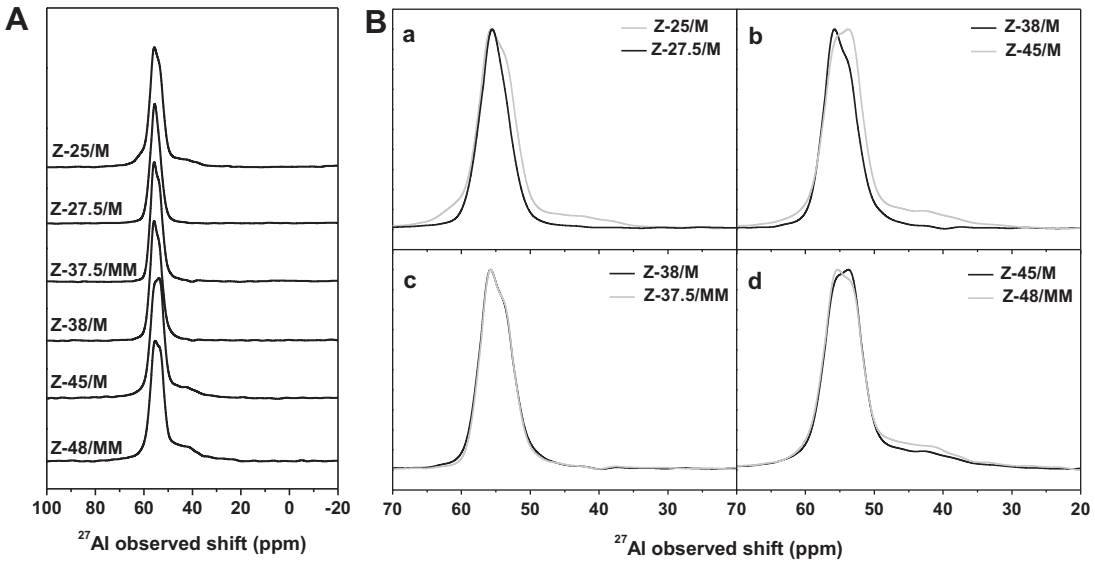

Fig. 1. (A) Normalised ^{27}Al MAS NMR spectra of hydrated Na-ZSM-5. (B) A comparison of (a) Z-25/M vs. Z-27.5/M, (b) Z-38/M vs. Z-45/M with similar Si/Al, (c) Z-38/M vs. Z-37.5/MM prepared by leaching, and (d) Z-45/M vs. Z-48/MM with mesoporosity generated by carbon templating.

corresponding Al species still remain a matter of discussion. The intensity increase at about 45 ppm was ascribed to less ordered Td framework Al atoms present in not-perfectly crystalline zeolites [37,52]. For steamed faujasites, Wouters et al. [49] explained the signals at 50–30 ppm by formation of gradually distorted Al tetrahedra and the subsequently developed signal at 30 ppm to formation of a fivefold coordinated Al atoms. A combined XRD, ^{29}Si and quantitative ^{27}Al MAS NMR analysis of steamed faujasites suggested, beside extra-framework Al species, also presence of perturbed Td coordinated Al atoms. Moreover, it was also shown that the intensity of the signals at 50–30 ppm does not reflect all the perturbed or partly released Al atoms [46]. Considering the above assignments given in the literature, the low intensity increase in the range of 50–30 ppm (with maximum at 45 ppm) observed for some samples in this study could only be qualitatively ascribed to variously perturbed framework Al species in the less ordered environment and/or partly removed Al species from the framework. It follows that the Z-27.5/M and Z-38/M samples did not contain significant concentration of perturbed tetrahedral Al sites, contrary to Z-25/M and Z-45/M. The alkaline and acid leaching of the Z-38/M sample (without Al defective sites) did not result in the appearance of defective sites in the Z-37.5/MM product. On the other hand, synthesis of micro-mesoporous Z-48/MM (carbon black template) of similar composition and conditions of synthesis as zeolite Z-45/M yielded a product with higher content of Al defective sites. Simulation of the spectra using Gaussian profiles both for the framework Al atoms in the region around 55 ppm (note that quadrupolar broadening can be neglected due to the highly symmetrical environment of Al atoms [43,44,53]) and for the perturbed Al species (the broad signal around 45 ppm represents rather an envelope of signals reflecting several perturbed Al species) was used to estimate the quantity of the perturbed Al atoms, as summarized in Table 3.

The absence of the perturbed framework Al atoms for Z-38/M and its micro-mesopore analogue Z-37.5/MM indicates that the alkaline treatment followed by acid leaching procedure has not generated perturbed Al sites. Extra-framework or perturbed Al species can be formed in the first step in the alkaline leaching, as reported in Ref. [9], but they are probably withdrawn from the sample by subsequent oxalic acid treatment [54]. In contrast to the micro-mesoporous Z-37.5/MM, the Z-48/MM zeolite prepared by synthesis using carbon template exhibited slightly higher concentration of perturbed Al-defective sites compared to the microporous Z-45/M sample. Such finding is not surprising if considered that a carbon template, occurring inside the zeolite was burned off in a final stage of synthesis. The released heat during high-temperature calcination could expectably induce local overheating and formation of the additional defective Al-sites [55].

Table 3
Framework defects in H-ZSM-5.

Sample	Perturbed tetrahedral Al[a] (%)	Al–OH[b]	Internal Si–OH [c]	c_L/c_{Al}	Al- and Si-framework defects
Z-25/M	5.5	Yes	Yes	0.13	High
Z-27.5/M	~0	Negligible	Negligible	0.09	Low
Z-37.5/MM	~0	No	Low	0.09	Low
Z-38/M	~0	No	Low	0.02	Low
Z-45/M	8.5	Yes	High	0.19	High
Z-48/MM	10.5	Yes	Very high	0.15	Very high

[a] From the broad signal centered at 45 ppm of the ^{27}Al MAS NMR spectra.
[b] From the IR band at 3650–70 cm^{-1}.
[c] From the IR band at 3727 cm^{-1}.

The analysis of the ^{27}Al MAS NMR spectra (Fig. 1) allows the following conclusions to be drawn: (i) the extra-framework Al with octahedral coordination was not present in any Na-zeolite sample, (ii) the tetrahedrally coordinated Al in the framework is exclusively present in Z-27.5/M, Z-37.5/MM and Z-38/M and (iii) a small part of framework Al (up to 10 rel. %) occurs as distorted Al tetrahedra forming framework defects, in the Z-25/M, Z-45/M and Z-48/MM samples.

3.3. Analysis of the FTIR spectra

The FTIR spectra of dehydrated H-ZSM-5 zeolites in the region of OH stretching vibrations exhibited two major bands at 3612 and 3745 cm^{-1} assigned to Brønsted sites and silanol groups, respectively (Fig. 2). In addition to these major bands, additional spectral components of lower intensity were found at 3727, around 3650–3670 cm^{-1} and a broad band around 3500 cm^{-1}. To better illustrate differences in the samples, the expanded spectra of selected pairs of samples Z-27.5/M vs. Z-25/M and Z-38/M vs. Z-45/M with a close Si/Al are compared in Fig. 3. The observed

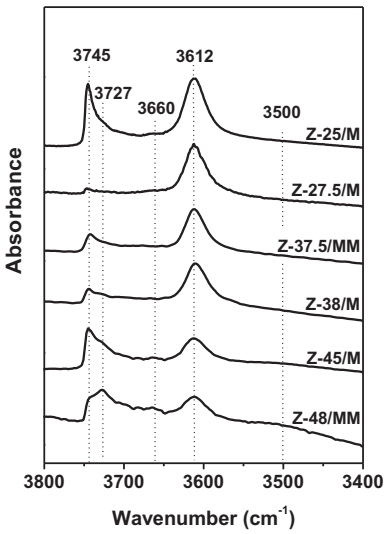

Fig. 2. FTIR spectra of micro and micro-mesoporous H-ZSM-5 dehydrated at 500 °C in the region of OH stretching vibrations.

absorptions of low intensity at about 3650–70 cm^{-1} have been ascribed to OH groups bound to extra-framework and/or perturbed framework Al atoms [56–58]. Different frequencies of the OH groups connected with the defective Al reflect various types of these Al sites. Zecchina et al. assigned the band at 3670 cm^{-1} to OH groups in ZSM-5 connected with partially extra-lattice Al positions with lower acid strength compared to structural OH groups [59,60]. It is to be also mentioned that these groups easily dehydroxylate and, therefore, the intensity of the absorption in the region 3650–70 cm^{-1} cannot be used as a quantitative measure of the extra-framework and/or perturbed framework Al atoms. Nevertheless, the IR absorption in the region 3650–3670 cm^{-1} for Z-25/M, Z-45/M and Z-48/MM matches the increased intensity of signals in the range 30–50 ppm observed in ^{27}Al MAS NMR spectra due to the presence of Al-related defective sites (cf. Figs. 1, 3 and 4). The intensity of the band at 3650–70 cm^{-1} is negligible or not observed for Z-27.5/M and Z-38/M indicating that Al atoms were incorporated nearly exclusively in the regular Td coordination in the framework as also observed by ^{27}Al MAS NMR.

Adsorption of d_3-acetonitrile was used for analysis of the concentration of Brønsted and Lewis sites in H-zeolites. The results of quantitative analysis of the bands at 2325 and 2297 cm^{-1} corresponding to the stretching mode of $\nu(C{\equiv}N)$ of d_3-acetonitrile adsorbed on Lewis and Brønsted sites, respectively, are listed in Table 1. A predominant concentration of Brønsted sites and low concentration of Lewis sites was found in the Z-27.5/M and Z-38/M samples. On contrary, the Z-25/M and Z-45/M samples with perturbed framework Al atoms and Al–OH groups exhibited more than 20 rel. % of Lewis sites. As the ^{27}Al MAS NMR spectra of all zeolites in hydrated Na-form did not detect octahedrally coordinated Al atoms, we can assume that in more flexible structure of the H-forms of ZSM-5 the Lewis sites are represented by the perturbed framework Al atoms. We have not straightforward evidences on the real structure of these Al-defective sites, neither they are available in the literature. The perturbed "framework" Al atoms can be formed by a step-wise weakening of the Al–OH bond in Si–OH–Al structural groups with formation of Si–OH groups. As the trigonal Al atoms are not stable they can be partly released from the framework and stabilized by terminal Al–OH groups. Some Lewis sites can also be created by partial zeolite dehydroxylation, when water molecule is formed from one structural OH group and a proton from another group. The mass balance of Al indicates that the loss of two Brønsted sites corresponds approximately to formation of one Lewis electron acceptor site (see Table 1). Thus, there are several mechanisms of formation of Lewis electron acceptor sites and several types of Al-perturbed sites can be formed.

The complexity of the spectrum of the silanol groups in H-ZSM-5 zeolites is most noticeable for the Z-45/M sample (Fig. 3). The main peak centred at 3745 cm^{-1}, shows a clear shoulder at lower frequency at about 3727 cm^{-1} and a broad band at 3500 cm^{-1} is observed in the spectrum. The bands at 3750–3700 cm^{-1} are generally associated with free Si–OH and an absorption with a maximum at about 3500 cm^{-1} with hydroxyls mutually interacting *via* hydrogen bonds [61]. It is to be noted that in the latter region the OH groups related to Al or structural Si–OH–Al groups can also be involved in such interactions, and therefore, the band at about 3500 cm^{-1} cannot be assigned exclusively to the interacting silanols. The component at about 3727 cm^{-1} has been attributed to free inner silanol groups located inside the zeolite crystal [61]. If we compare the spectra of Z-45/M and Z-38/M, it is obvious that Z-45/M exhibits much higher intensity of the bands of both surface

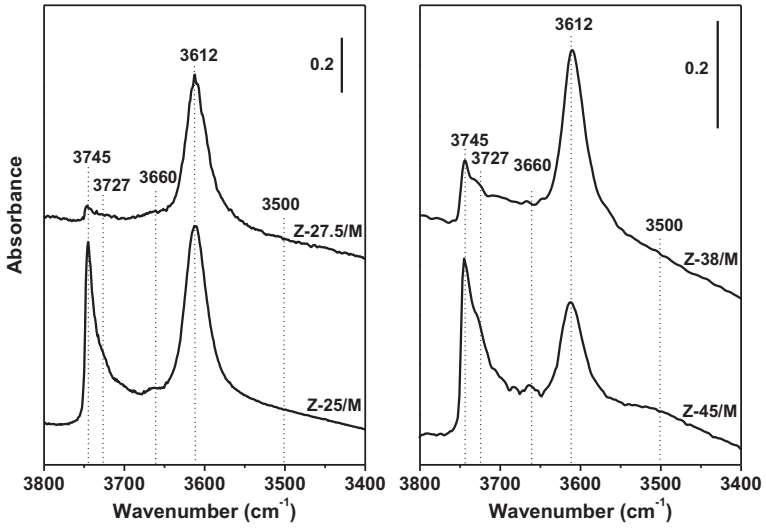

Fig. 3. Comparison of the FTIR spectra of microporous H-ZSM-5 dehydrated at 500 °C.

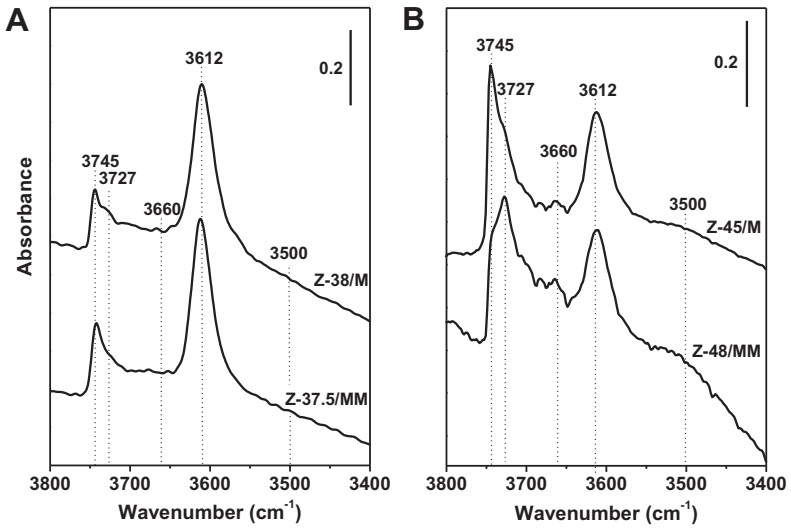

Fig. 4. Comparison of the FTIR spectra of microporous H-ZSM-5 dehydrated at 500 °C and their micro-mesoporous analogues prepared by (A) the leaching procedures and (B) using secondary carbon template.

and internal silanol defects (Fig. 3). Also Z-25/M compared to Z-27.5/M (Fig. 3) shows the most obvious difference in much higher intensity of the bands at 3745 and 3727 cm^{-1}, indicating the presence of high concentrations of both the external and internal silanols. It should be noted that Z-25/M is composed of crystals of 0.5 μm compared to the 3 μm crystals of Z-27.5/M that explain the substantial difference of the intensities of the band of Si–OH groups on an external surface. The analysis of the FTIR spectra can be summarised as follows (see Table 3). Z-27.5/M and Z-38/M exhibit terminal silanol groups, structural Brønsted OH groups and very low amount of internal silanols, as typical for low-defective zeolites, while the Z-25/M and Z-45/M samples exhibit in addition internal defects containing silanol nests, typical for defective framework.

Fig. 4 compares FTIR spectra of OH groups of samples with mesoporosity generated by different methods. Part A shows the spectra of Z-38/M and its micro-mesoporous analogue Z-37.5/MM prepared by alkaline and oxalic acid leaching. The leaching procedure led to an increase in the intensity of the band at 3745 cm^{-1} due to terminal silanols in the formed mesopores, whereas bands at 3727, 3650–70 (and 3500) cm^{-1}, which can be associated with defective OH sites, did not change (or slightly decreased) their intensity. Therefore, the alkaline and acid leaching procedure led to the formation of mesopores with their surface similar to the external surface of the zeolite crystal and neither new Al- nor Si-related OH internal defective sites were formed.

A comparison of the spectra of Z-45/M and its analogue Z-48/MM with mesoporosity generated by the carbon templating is shown in Fig. 4B. The most remarkable difference to the micro-mesoporous zeolite Z-37.5/MM obtained by leaching procedure and to analogue Z/45/M is higher evolution of the high intensity of the dominating band at 3727 cm^{-1} and that of 3500 cm^{-1} as well as in the region 3650–70 cm^{-1}. These findings show a high abundance of defective sites in micro-mesoporous zeolite prepared by black carbon templating, i.e., formation of distorted tetrahedral Al framework atoms, manifested in ^{27}Al MAS NMR spectra (Fig. 1) and higher concentration of electron acceptor Lewis sites (Table 1), increased amount of free inner silanols (3727 cm^{-1}) and nests of hydrogen-bonded silanols (3500 cm^{-1}). The increased amount of silanols (free and interacting) might be formed in the walls of mesopores during burning off carbon particles. It is obvious that the direct synthesis of micro-mesoporous ZSM-5 by carbon templating resulted in highly defective zeolitic structure compared to that prepared by the alkaline/acid leaching procedure.

3.4. Effect of framework defects on MTH over ZSM-5

3.4.1. Microporous H-ZSM-5 zeolites

It is well known that both the selectivity and the deactivation of H-ZSM-5 catalyst in MTH process depends on a number of variables, such as number and strength of acid sites, geometry of channels, crystal size as well as reaction conditions. Therefore, we attempted to compare zeolite samples exhibiting similar framework composition and crystal size. We selected two pairs of samples, ZSM-25/M vs. Z-27.5/M (Si/Al 25 and 27.5, respectively) and Z-38/M vs. Z-45/M (Si/Al of 38 and 45, respectively) in which the samples significantly differ in the concentration of defective sites, as revealed by ^{27}Al MAS NMR, FTIR spectra of OH groups and C≡N groups of adsorbed d_3-acetonitrile. Yields of ethene and propene, C_1–C_3 paraffins, butenes, butanes and C_6^+ hydrocarbons comprising aromatics were obtained, and are given in Fig. 5. It is seen for both pairs of microporous H-ZSM-5 that the low-defective ones compared to slightly defective samples with close framework composition result in higher yields of propene, ethene and butenes and lower yields of paraffins and C_6^+ hydrocarbons. On contrary, the higher content of framework defects in zeolites favours the formation of C_6^+ hydrocarbons and butanes. Thus, the results show that the presence of framework defects enhances hydrogen transfer reactions leading to aromatics and paraffins at the expense of the C_2 and C_3 olefins.

The pairs of Z-25/M vs. Z-27/M and Z-38/M vs. Z-45/M samples exhibited small crystals around 0.5 μm (with exception of Z-27/M – 3.0 μm) for which differences in the diffusion rate of reactants could be neglected. Therefore, they seemed suitable for analysis of the effect of the presence of framework defects on the yield of the individual products. However, the yields of the individual products for Z-27.5/M with crystal size of 3 μm could be considered to be affected by intra-crystalline diffusion, but Chen et al. have shown for SAPO-34 that the selectivity for olefins is almost independent on crystal size in the range 0.5–2.5 μm [62]. Nevertheless, it was found for much larger crystals of H-ZSM-5 that the intermolecular hydride transfer reactions, leading to the formation of aromatics and alkanes, were enhanced compared to the smaller crystal size zeolites [3]. This finding is a result of the

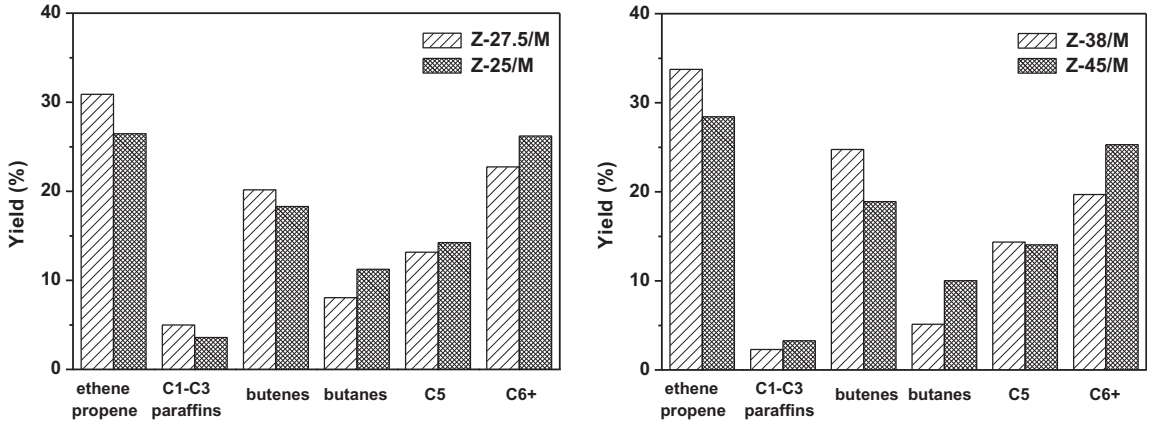

Fig. 5. Effect of the framework defective sites in microporous H-ZSM-5 on the yield of products in MTH. T = 370 °C, WHSV = 20 h^{-1}.

longer contact time in large crystals compared to small ones. Fig. 5 shows higher yields of aromatics and alkanes for the defective Z-25/M sample with smaller crystals (0.5 μm) compared to the non-defective Z-27.5/M with larger crystals (3 μm). Therefore, this result clearly manifests that the Al- and Si-defective framework is responsible for the higher yields of aromatics and alkanes and lower yields of olefins.

3.4.2. Micro-mesoporous ZSM-5 zeolites

The effect of framework defective sites in zeolites with mesoporous structure on their selectivity and durability in MTH was analysed on the zeolites prepared by the alkaline/acid leaching and by the carbon templating procedures. A comparison of the yield of products and conversion of methanol to hydrocarbons as a function of time over the low-defective microporous Z-38/M

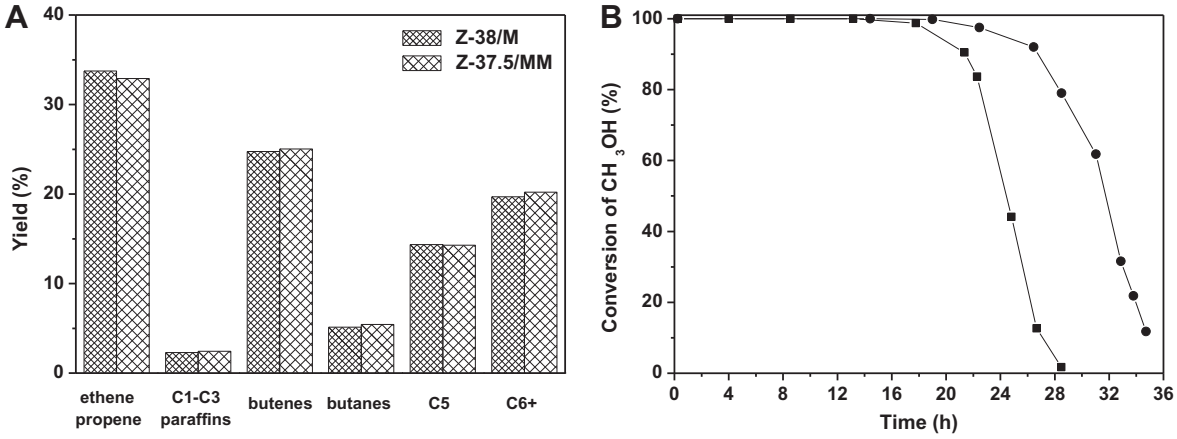

Fig. 6. (A) Yield of hydrocarbons at TOS of 20 min and (B) conversion of methanol to hydrocarbons as a function of TOS over Z-38/M (–■–) and Z-37.5/MM prepared by the leaching procedures (–●–). T = 370 °C, WHSV = 20 h^{-1}.

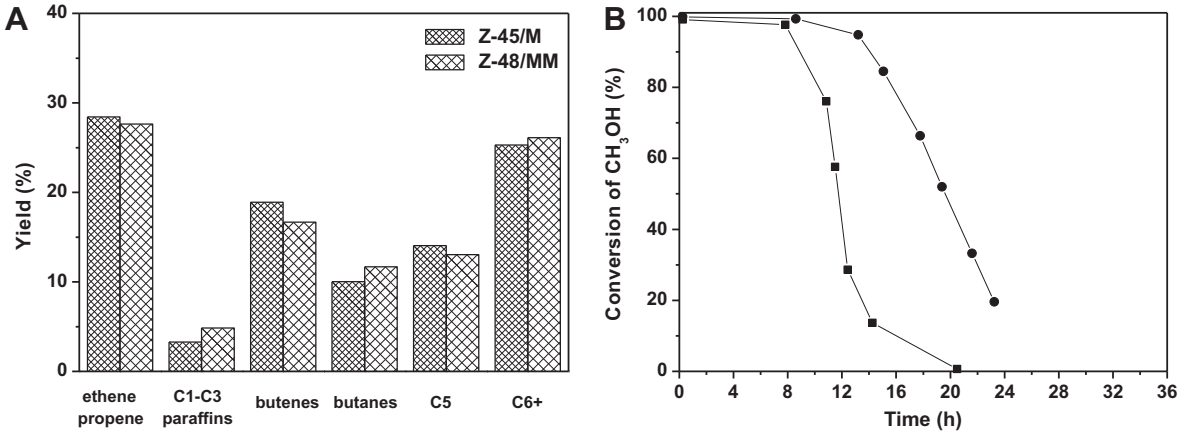

Fig. 7. (A) Yield of hydrocarbons at TOS of 20 min and (B) conversion of methanol to hydrocarbons as a function of TOS over Z-45/M(–●–) and Z-48/MM (–■–) prepared by using secondary carbon template. T = 370 °C, WHSV = 20 h^{-1}.

and the micro-mesoporous Z-37.5/MM sample prepared by leaching of the former one is shown in Fig. 6A and B. An almost insignificant decrease in the yield of propene and ethene and a corresponding small increase in the yield of low paraffins and C_6^+ hydrocarbons were observed after the formation of mesopores. On contrary to the product distribution, which was practically not altered by such mesoporosity, deactivation of the catalysts was significantly suppressed with micro-mesoporous Z-37.5/MM. The conversion of methanol to hydrocarbons decreased to a level of 50% at TOS of 24 h over Z-38/M, while the micro-mesoporous Z-37.5/MM zeolite maintained conversion over 50% for 32 h of TOS. The improvement in the catalyst life-time is in agreement with the observation in Ref. [9] testing methanol to hydrocarbon reaction over microporous and micro-mesoporous H-ZSM-5, but not analyzing the structure and properties of Si- and Al-related defective sites.

The yield of products and conversion of methanol to hydrocarbons as a function of time for microporous Z-45/M and the more defective micro-mesoporous analogue (Z-48/MM), prepared by burning off the incorporated carbon particles after the hydrothermal synthesis, is compared in Fig. 7. The micro-mesoporous zeolite provided only slightly higher yields of paraffins and C_6^+ hydrocarbons at the expense of C_2–C_4 olefins. However, in comparison with the less defective microporous zeolite Z-45/M, it underwent very rapid deactivation. The conversion of methanol to hydrocarbons over Z-48/MM dropped to 50% already at TOS of 12 h, while microporous Z-45/M maintained methanol conversion over 50% for TOS of 20 h. Therefore, the developed secondary mesoporosity by carbon addition into the synthesis gel under conditions reported here did not produce an improvement in the stability of the catalyst activity in the MTH reaction.

4. Discussion

The analysis of Al coordination by ^{27}Al MAS NMR and the FTIR spectral characteristics of the OH groups (structural Si–OH–Al, Al–OH, external and internal Si–OH) and C≡N groups of adsorbed d_3-acetonitrile on strong acid Brønsted OH groups and Lewis electron acceptor sites could provide a complementary insight into the structure of such defects. Nevertheless, we had well in mind that some of the spectral characteristics (external and internal Si–OH and Al–OH groups) could not be analysed quantitatively because of the absence of extinction coefficients and/or contribution of several species to them. On contrary, the concentration of Si–OH–Al groups, extra-framework Al species and Lewis electron acceptor sites could be well-estimated. To attempt understanding of the structure and role of Si- and Al-related defective sites in the framework of ZSM-5 in the MTH process, we selected zeolites with similar basic structural parameters, such as Si/Al and crystal size, but different degree of "defectivity" formed during the synthesis of microporous zeolites and zeolites with hierarchic micro-mesoporosity.

4.1. Framework defects and MTH reaction over microporous ZSM-5 zeolites

The selected H-ZSM-5 samples, exhibiting according to XRD and sorption measurements regular microporous MFI structure (Table 1), contained different amount of defective sites. Only the characteristic IR vibration of bridging OH groups (3612 cm^{-1}) without significant intensity at 3650–70 cm^{-1} related to vibrations of hydroxyls on Al atoms, have been found in the FTIR spectra (Figs. 2 and 3) for Z-27.5/M and Z-38/M, indicating practically all Al atoms in the framework in regular Td coordination, involved in structural Si–OH–Al groups, and negligible concentration of Lewis sites (Table 1). This finding agrees with the absence of distorted Al tetrahedra with these samples (^{27}Al MAS NMR signal at 30–50 ppm, Fig. 1), and presence of exclusively Td coordinated Al atoms (55, 57 and 61 ppm, see Fig. 1 and Table 3). In agreement with the absence of Al-defective sites, also low amount of internal silanols were present in these zeolites. In contrast to these highly regular H-ZSM-5 zeolites, the Z-25/M and Z-45/M samples exhibited low, but significant amount (estimated 5–8% of Al) of perturbed Td coordinated Al atoms as indicated by a clearly seen increase in intensity of the NMR signal at 30–50 ppm (Fig. 1, Table 3), IR absorption intensity at 3650–70 cm^{-1} of Al–OH (Fig. 3) and high concentration of Lewis sites (Table 1). Development of the internal silanols inside the crystals of the defective samples shows that the defective sites at the Al environment are balanced by formation of adjacent free internal silanol groups (Fig. 3).

Thus, the analysis of the effect of framework defects on the MTH reaction has been done on the highly ordered zeolites, exhibiting no-measurable or negligible amount of defective Al- and Si-related sites, and on zeolites (although exhibiting regular microporous structure according to XRD and micropore volume) containing low concentration of Al- and Si-defective sites such as usually occurring in commercial, but also in samples synthesized in the laboratory. As the concentration of defective sites was low and the crystal size around 0.5 μm (3.0 μm only for Z-27.5/M) we did not expect significant differences in mass transport among the individual zeolite samples, like that reported for severely steamed zeolites with high content of extra-framework Al species and amorphous phase [63].

Occurrence of the defective Al- and Si-related sites is manifested in the selectivity of methanol transformation to hydrocarbons (Fig. 5). The non-defective highly ordered Z-27.5/M and Z-38/M samples compared to defective Z-25/M and Z-45/M ones, respectively, provide higher yields of low olefins and lower yields of aromatics and paraffins. The results are convincing, although the former couple of samples differ in crystal size (Fig. 5, Table 1) and the latter couple in the concentration of Brønsted sites (Fig. 5, Table 1). As already mentioned larger crystals and higher concentration of Brønsted sites enhance hydrogen transfer reactions with aromatization and paraffin formation [61,64]. Therefore, the effect of defects on the MTH selectivity might be even higher for samples strictly identical in the crystal size and composition.

As it is well-documented that the acid strength of Brønsted sites in H-ZSM-5 is equal regardless of Si/Al composition [5–9] and the MTH, as a consecutive reaction, governed by their concentration, we consider the differences in selectivity for defective and non-defective zeolites of similar Si/Al composition to be caused by the contribution of defective sites. It is seen that even such low concentration of defective sites (~10 rel. % of total Al), which are usually present not only in commercial zeolites, but also in those carefully synthesized in the laboratory, changes the selectivity of MTH reaction in the direction of enhancement of the aromatization and hydrogen transfer reactions. As previously found out by us and others [64–68] the presence of Al-related electron acceptor sites in H-ZSM-5 supports oligomerization and hydrogen transfer reactions leading to coke formation, as demonstrated for numerous acid catalyzed reactions of hydrocarbons. Nevertheless, the effect of the Lewis electron acceptor sites on the acid-catalyzed reactions is not so far satisfactory elucidated. The suggested increased strength of the Brønsted sites next to Lewis sites [69,70] was not clearly proven, and the mechanism of the probable direct function of Lewis sites has also not been explained.

4.2. Framework defects and MTH reaction over micro-mesoporous H-ZSM-5

The micro-mesoporous Z-37.5/MM and Z-48/MM differed, besides the concentration of Brønsted sites, not only in the

concentration of defective Al- and Si-related sites (Table 3), but also in the completely different ways of their preparations. This could naturally lead to different location and accessibility of the mesopores to reactants. Nevertheless, the mesopore and micropore volumes for these samples were close and also their crystal size (see Table 1).

A high abundance of internal silanols (3727 cm^{-1}) and higher occurrence of perturbed Td coordinated framework Al atoms (Fig. 1), Al–OH (Fig. 4B) and Lewis sites (Table 1) was characteristic for the micro-mesoporous Z-48/MM zeolite, synthesized by using carbon particles, compared to microporous Z-45/M analogue. In this synthesis, zeolite framework is formed around the carbon particles [31–38], and mesopores are generated after burning off the carbon. The micropore volume of Z-48/MM was well-developed (see V_{MI} in Table 2), but we have no information on the inter-connectivity of the mesopores. A possible local over-heating could lead to a partial destruction of a thin layer of the zeolite forming mesopores. This could cause the observed increase in internal silanols, perturbed Al atoms, and Al–OH namely in vicinity of the surface of mesopores.

On contrary to micro-mesoporous H-ZSM-5 prepared by using carbon template particles in the zeolite synthesis, the micro-mesoporous Z-37.5/MM zeolite prepared by alkaline followed by oxalic acid leaching contained very low amount of both, internal silanols, Al–OH (Fig. 4), perturbed framework Al atoms (Fig. 1), and Lewis sites (Table 1). Thus the latter procedure of mesopores development led unambiguously to micro-mesoporous structure practically without defective sites.

Groen et al. [24] by analysing a series of H-ZSM-5 of various Si/Al compositions have revealed that the optimum for framework desilication and mesopore formation is concentration of framework Al of 1.9–3.8 Al/u.c., i.e., of Si/Al 25–50. They suggested that framework Al atoms stabilize the structure against alkaline leaching and mesopores are created by desilication of a part of the zeolite free of Al. They showed that too low Al content results in a massive dissolution of zeolites with creation of large meso- and macropores. The Z-38/M zeolite sample falls into the "optimum" Al concentration range, and the volume of mesopores obtained in Z-38/MM was 0.15 $cm^3\ g^{-1}$. Recent analysis of structural Si–OH–Al, Lewis sites, and internal and external Si–OH groups in large (15 μm) crystals of H-ZSM-5 crystals those after alkaline leaching by means of adsorption of differently sterically demanded probe molecules, as CO and voluminous collidine, revealed that in alkaline leached zeolites the Lewis sites were present not only on the original crystal surface, but also in the developed mesopores, while the internal silanols decreased in their concentration [9]. The decrease in internal silanols for micro-mesoporous Z-38/MM zeolite can be therefore accounted for desilication of the inner Si-defects from the parent Z-37.5/M sample. It is to be pointed out that the further treatment of the desilicated zeolite by oxalic acid can be expected to result in an elution of the extra-framework Al species.

With respect to the MTH reaction, formation of mesopores in both the micro-mesopore H-ZSM-5 zeolites, differing substantially in the way of their preparation, and compared to their analogues, caused only a slight changes in selectivity to higher olefins, paraffins and aromatics (Figs. 6 and 7). However, the life-time of the micro-mesoporous zeolite, prepared by templating with carbon particles in its synthesis, was substantial shorter compared to the corresponding analogue (12 vs. 20 h at 50% conversion, Fig. 7). This increased coking of the micro-mesoporous zeolite might be connected with the higher concentration of defective Al- and Si-sites, particularly in or close to the mesopore surface, although contribution of the expected occurrence of not inter-connected inner void volumes should also be considered.

On contrary, the life-time of the alkaline and subsequently acid leached Z-37.5/MM, compared to the parent sample, was substantially increased (Fig. 6), indicating lower extent of formation of voluminous polyalkyl (poly)aromatics. This finding, together with the nearly exclusive presence of structural Si–OH–Al groups and practically absence of the Al- and Si-defective sites in this micro-mesoporous zeolite, implies that the mesopore surface likely do not contains strong acid and Al- and Si-defective sites. Moreover, the mesopore inter-connected structure and surface with minimum concentration of strong acid sites enables fast desorption and transport of voluminous aromatics from the zeolite pores.

It is to be noted that the micro-mesoporous zeolite prepared by templating with carbon particles exhibited ca 3x shorter life-time (cf. Figs. 6 and 7), due to Al- and Si-defective sites and likely of not inter-connected inner mesopores, compared to the defect free micro-mesoporous zeolite obtained by alkaline and acid leaching.

5. Conclusions

Both the H-ZSM-5, commercial and those synthesized in the laboratory, with highly regular XRD structure and well-developed micropore volume, often contain in the framework low concentration of Al- and Si-related defective sites. Analysis of the structure of these species by ^{27}Al MAS NMR, FTIR spectra of OH groups and C≡N groups of adsorbed d_3-acetonitrile, revealed prevailing concentration of framework structural Si–OH–Al groups with Td coordinated Al atoms, absence of extra-framework regularly Oh coordinated Al, low concentration of Al–OH groups, perturbed Td coordinated framework Al atoms and electron acceptor Lewis sites, and presence of external and internal silanol groups. It has been shown that even low concentration of Al- and Si-related defective sites in H-ZSM-5 substantially affects the product composition and stability of conversion during methanol transformation to hydrocarbons. The low-defective highly ordered H-ZSM-5 favours formation of C_2 and C_3 olefins on the account of the C_1–C_4 paraffins and aromatics. On contrary, the zeolites with defective sites enhance hydrogen transfer reactions leading to higher selectivity to aromatics and paraffins.

It has been demonstrated that the formation of mesoporosity by introduction of carbon particles during the synthesis of ZSM-5 leads to a significant concentration of perturbed framework Al atoms, formation of Al–OH species, Lewis electron acceptor sites and internal silanols, mostly close to mesopores. Presence of such defective sites resulted in a half life-time of H-ZSM-5 due to coke formation, compared to a microporous analogue. On contrary, creation of mesopores by zeolite desilication by alkaline treatment (removing a part of the zeolite containing internal silanols) and subsequent leaching of perturbed framework aluminium (Al-Lewis sites, Al–OH) by oxalic acid resulted in non-defective highly regular micro-mesoporous structure. It provided at the same concentration of Brønsted sites similar selectivity as the parent microporous zeolite, but a high advantage of micro-mesoporous H-ZSM-5 prepared by alkaline and acid leaching was its substantially long life-time in the MTH reaction.

Acknowledgments

This study was supported by the Czech Science Foundation under the project # GP 203/08/P593 and Grant Agency of the Academy of Sciences of the Czech Republic under the projects # IAA400400812 and IAA400400904.

References

[1] C.D. Chang, A.J. Silvestri, J. Catal. 47 (1977) 249–259.
[2] C.D. Chang, Catal. Rev. 25 (1983) 1–118.
[3] M. Stöcker, Microporous Mesoporous Mater. 29 (1999) 3–48.
[4] F.J. Keil, Microporous Mesoporous Mater. 29 (1999) 49–66.
[5] D.H. Olson, W.O. Haag, R.M. Lago, J. Catal. 61 (1980) 390–396.

[6] D.H. Olson, W.O. Haag, ACS Symp. Ser. 248 (1984) 275–307.
[7] T. Armaroli, L.J. Simon, M. Digne, T. Montanari, M. Bevilacqua, V. Valtchev, J. Patarin, G. Busca, Appl. Catal., A 306 (2006) 78–84.
[8] P. Sazama, J. Dedecek, V. Gabova, B. Wichterlova, G. Spoto, S. Bordiga, J. Catal. 254 (2008) 180–189.
[9] M.S. Holm, S. Svelle, F. Joensen, P. Beato, C.H. Christensen, S. Bordiga, M. Bjørgen, Appl. Catal., A 356 (2009) 23–30.
[10] I.M. Dahl, S. Kolboe, Catal. Lett. 20 (1993) 329–336.
[11] I.M. Dahl, S. Kolboe, J. Catal. 149 (1994) 458–464.
[12] I.M. Dahl, S. Kolboe, J. Catal. 161 (1996) 304–309.
[13] J.F. Haw, W. Song, D.M. Marcus, J.B. Nicholas, Acc. Chem. Res. 36 (2003) 317–326.
[14] W. Wang, A. Buchholz, M. Seiler, M. Hunger, J. Am. Chem. Soc. 125 (2003) 15260–15267.
[15] W. Wang, Y. Jiang, M. Hunger, Catal. Today 113 (2006) 102–114.
[16] Z.M. Cui, Q. Liu, W.G. Song, L.J. Wan, Angew. Chem. Int. Ed. 45 (2006) 6512–6515.
[17] M. Bjørgen, S. Svelle, F. Joensen, J. Nerlov, S. Kolboe, F. Bonino, L. Palumbo, S. Bordiga, U. Olsbye, J. Catal. 249 (2007) 195–207.
[18] M. Bjørgen, F. Joensen, K.P. Lillerud, U. Olsbye, S. Svelle, Catal. Today 142 (2009) 90–97.
[19] H. Schulz, Catal. Today 154 (2010) 183–194.
[20] C.M. Wang, Y.D. Wang, H.X. Liu, Z.K. Xie, Z.P. Liu, J. Catal. 271 (2010) 386–391.
[21] M. Bjørgen, S. Akyalcin, U. Olsbye, S. Benard, S. Kolboe, S. Svelle, J. Catal. 275 (2010) 170–180.
[22] D. Mores, E. Stavitski, M.H.F. Kox, J. Kornatowski, U. Olsbye, B.M. Weckhuysen, Chem. Eur. J. 14 (2008) 11320–11327.
[23] J.C. Groen, J.C. Jansen, J.A. Moulijn, J. Pérez-Ramírez, J. Phys. Chem. B 108 (2004) 13062–13065.
[24] J.C. Groen, J.A. Moulijn, J. Pérez-Ramírez, J. Mater. Chem. 16 (2006) 2121–2131.
[25] J.C. Groen, T. Sano, J.A. Moulijn, J. Pérez-Ramírez, J. Catal. 251 (2007) 21–27.
[26] J.C. Groen, W. Zhu, S. Brouwer, S.J. Huynink, F. Kapteijn, J.A. Moulijn, J. Perez-Ramirez, J. Am. Chem. Soc. 129 (2007) 355–360.
[27] J.C. Groen, G.M. Hamminga, J.A. Moulijn, J. Pérez-Ramírez, Phys. Chem. Chem. Phys. 9 (2007) 4822–4830.
[28] B. Gil, L. Mokrzycki, B. Sulikowski, Z. Olejniczak, S. Walas, Catal. Today 152 (2010) 24–32.
[29] L. Sommer, D. Mores, S. Svelle, M. Stöcker, B.M. Weckhuysen, U. Olsbye, Microporous Mesoporous Mater. 132 (2010) 384–394.
[30] C. Choifeng, J.B. Hall, B.J. Huggins, R.A. Beyerlein, J. Catal. 140 (1993) 395–405.
[31] S. Van Donk, A.H. Janssen, J.H. Bitter, K.P. De Jong, Catal. Rev. Sci. Eng. 45 (2003) 297–319.
[32] C.J.H. Jacobsen, C. Madsen, J. Houzvicka, I. Schmidt, A. Carlsson, J. Am. Chem. Soc. 122 (2000) 7116–7117.
[33] A.H. Janssen, I. Schmidt, C.J.H. Jacobsen, A.J. Koster, K.P. de Jong, Microporous Mesoporous Mater. 65 (2003) 59–75.
[34] M. Hartmann, Angew. Chem. Int. Ed. 43 (2004) 5880–5882.
[35] Y.H. Chou, C.S. Cundy, A.A. Garforth, V.L. Zholobenko, Microporous Mesoporous Mater. 89 (2006) 78–87.
[36] Z. Pavlackova, G. Kosova, N. Silkova, A. Zukal, J. Cejka, Scientific bases for the preparation of heterogeneous catalysts, in: E.M. Gaigneaux, M. Devillers, S. Hermans, P. Ruiz, D.E. Vos, P.A. Jacobs, J.A. Martens (Eds.), Studies in Surface Science and Catalysis, vol. 162, 2006, pp. 905–912.
[37] J.-B. Koo, N. Jiang, S. Saravanamurugan, M. Bejblova, Z. Musilová, J. Cejka, S.-E. Park, J. Catal. 276 (2010) 327–334.
[38] Z. Musilova, N. Zilkova, S.E. Park, J. Cejka, Top. Catal. 53 (2010) 1457–1469.
[39] P. Kortunov, S. Vasenkov, J. Kärger, R. Valiullin, P. Gottschalk, M.F. Elía, M. Perez, M. Stöcker, B. Drescher, G. McElhiney, C. Berger, R. Gläser, J. Weitkamp, J. Am. Chem. Soc. 127 (2005) 13055–13059.
[40] M. Bjørgen, F. Joensen, M. Spangsberg Holm, U. Olsbye, K.P. Lillerud, S. Svelle, Appl. Catal. Gen. 345 (2008) 43–50.
[41] C.H. Christensen, K. Johannsen, I. Schmidt, C.H. Christensen, J. Am. Chem. Soc. 125 (2003) 13370–13371.
[42] B. Wichterlova, Z. Tvaruzkova, Z. Sobalik, P. Sarv, Microporous Mesoporous Mater. 24 (1998) 223–233.
[43] S. Sklenak, J. Dedecek, C. Li, B. Wichterlova, V. Gabova, M. Sierka, J. Sauer, Angew. Chem. Int. Ed. 46 (2007) 7286–7289.
[44] S. Sklenak, J. Dedecek, C. Li, B. Wichterlova, V. Gabova, M. Sierka, J. Sauer, Phys. Chem. Chem. Phys. 11 (2009) 1237–1247.
[45] J. Dedecek, S. Sklenak, C. Li, B. Wichterlova, V. Gabova, J. Brus, M. Sierka, J. Sauer, J. Phys. Chem. C 113 (2009) 1447–1458.
[46] M.J. Remy, D. Stanica, G. Poncelet, E.J.P. Feijen, P.J. Grobet, J.A. Martens, P.A. Jacobs, J. Phys. Chem. 100 (1996) 12440–12447.
[47] T.H. Chen, B. Wouters, P. Grobet, Chem. J. Internet 2 (2000) 7–13.
[48] T.H. Chen, B.H. Wouters, Eur. J. Inorg. Chem. (2000) 281–285.
[49] B.H. Wouters, T. Chen, P.J. Grobet, J. Phys. Chem. B 105 (2001) 1135–1139.
[50] J. Chen, T. Chen, N. Guan, J. Wang, Catal. Today 93–95 (2004) 627–630.
[51] A. Samoson, E. Lippmaa, G. Engelhardt, U. Lohse, H.G. Jerschkewitz, Chem. Phys. Lett. 134 (1987) 589–592.
[52] T.O. Do, A. Nossov, M.A. Springuel-Huet, C. Schneider, J.L. Bretherton, C.A. Fyfe, S. Kaliaguine, J. Am. Chem. Soc. 126 (2004) 14324–14325.
[53] D.M. Roberge, H. Hausmann, Phys. Chem. Chem. Phys. 4 (2002) 3128–3135.
[54] R. Caicedo-Realpe, J. Pérez-Ramírez, Microporous Mesoporous Mater. 128 (2010) 91–100.
[55] I. Jirka, P. Sazama, A. Zikanova, P. Hrabanek, M. Kocirik, Microporous Mesoporous Mater. 137 (2011) 8–17.
[56] M.B. Sayed, R.A. Kydd, R.P. Cooney, J. Catal. 88 (1984) 137–149.
[57] L.M. Kustov, V.B. Kazansky, S. Beran, L. Kubelkova, P. Jiru, J. Phys. Chem. 91 (1987) 5247–5251.
[58] P.O. Fritz, J.H. Lunsford, J. Catal. 118 (1989) 85–98.
[59] A. Zecchina, S. Bordiga, G. Spoto, D. Scarano, G. Petrini, G. Leofanti, M. Padovan, C.O. Arean, Faraday Trans. 88 (1992) 2959–2969.
[60] R. Buzzoni, S. Bordiga, G. Ricchiardi, C. Lamberti, A. Zecchina, G. Bellussi, Langmuir 12 (1996) 930–940.
[61] S. Bordiga, I. Roggero, P. Ugliengo, A. Zecchina, V. Bolis, G. Artioli, R. Buzzoni, G. Marra, F. Rivetti, G. Spano, C. Lamberti, Dalton Trans. (2000) 3921–3929.
[62] D. Chen, K. Moljord, T. Fuglerud, A. Holmen, Microporous Mesoporous Mater. 29 (1999) 191–203.
[63] J.S. Buchanan, D.H. Olson, S.E. Schramm, Appl. Catal., A 220 (2001) 223–234.
[64] O. Bortnovsky, P. Sazama, B. Wichterlova, Appl. Catal., A 287 (2005) 203–213.
[65] A. Corma, J. Planelles, J. Sánchez-Marín, F. Tomás, J. Catal. 93 (1985) 30–37.
[66] B. Wichterlová, N. Zilkova, E. Uvarova, J. Cejka, P. Sarv, C. Paganini, J.A. Lercher, Appl. Catal., A 182 (1999) 297–308.
[67] B. Wichterlová, J. Cejka, Catal. Rev. Sci. Eng. 44 (2002) 375–421.
[68] H. Matsuura, N. Katada, M. Niwa, Microporous Mesoporous Mater. 66 (2003) 283–296.
[69] C. Mirodatos, J. Chem. Soc., Chem. Commun. (1981) 39–40.
[70] A. Corma, A. Martínez, P.A. Arroyo, J.L.F. Monteiro, E.F. Sousa-Aguiar, Appl. Catal., A Gen. 142 (1996) 139–150.